Journal of Process Control 159 (2026) 103638

Contents lists available at ScienceDirect

Journal of Process Control

journal homepage: www.elsevier.com/locate/jprocont

Efficient learning-based predictive control for acid gas abatement in waste to energy processes☆

Andrea Wu [a], Andres Cordoba-Pacheco [b], Senem Ozgen [a], Fredy Ruiz [b,*]

[a] LEAP (Laboratorio Energia Ambiente Piacenza), Piacenza, Italy
[b] Dipartimento di Elettronica, Informazione e Bioingegneria, Politecnico di Milano, Milan, Italy

ARTICLE INFO

Keywords:
Adaptive model predictive control
Data-driven control
Set membership estimation
Waste to energy plants
Flue gas treatment

ABSTRACT

Waste-to-energy plants have become a strategic resource to reduce the volume of non-recyclable solid waste in municipalities. Flue gas treatment is a key component in making these plants clean and sustainable. In particular, acid gas abatement is a fundamental process for complying with emission standards. However, developing models of the abatement process is challenging due to the complexity of the phenomena and reactions occurring inside the pollutant abatement system. In this work, a predictive control strategy is proposed to regulate the concentration of hydrogen chloride in the flue gas of a waste-to-energy plant by manipulating the reactant flow rate. Black-box models for simulation and prediction tasks are derived from experimental data from a real WtE plant in Italy. A learning strategy is proposed to update an autoregressive model of the process in real-time using Set Membership identification techniques, and a Model Predictive Controller is formulated to optimally manipulate the reactant feed rate, guaranteeing that emissions comply with regulatory constraints while minimizing the reactant dosage. The performance of the resulting control strategy is compared with a standard PI plus FeedForward controller, currently employed in this kind of process. The results show that the adaptive MPC improves the tracking performance, reducing the Mean Integrated Absolute Error by up to 57.1% and reactant consumption by 3%, while ensuring better compliance with emission regulations.

1. Introduction

Handling municipal solid waste is a complex task, particularly in densely populated areas where large volumes of waste are produced daily [1]. One of the most established and scalable solutions for waste treatment is incineration in Waste-to-Energy (WtE) plants, where municipal waste is converted into electrical and thermal energy. However, WtE plants are complex industrial systems that generate flue gases containing harmful and polluting compounds, such as hydrogen chloride (HCl), which must be effectively treated to meet environmental standards [2].

Effective control of acid gas abatement in WtE systems relies heavily on accurate process models. However, modeling these systems is particularly challenging due to their nonlinear behavior, plant-to-plant variability, and the strong interdependence among subsystems and process variables [3]. Traditional physics-based models, although theoretically grounded, often describe only isolated components of the process and require simplifying assumptions that compromise accuracy and generalizability [4].

Diverse physics-based models have been proposed to characterize specific mechanisms within the abatement system, including steady-state models for reagent comparison [5], shrinking core reaction models in bag filters [6], and in-duct sorbent injection models [7]. Some models have been adapted specifically for hydrochloric acid removal [8,9]. Despite their insights, these models are typically limited to small process segments and cannot be easily validated due to sparse sensor coverage, which restricts real-time observation to points upstream and downstream of the abatement system [10–12].

To address these limitations, black-box, data-driven modeling approaches have gained traction [13]. Unlike physics-based models, black-box models focus purely on the dynamic relationships between

☆ This research has been partially supported by the Italian Ministry of University and Research under grant "Learning-based Model Predictive Control by Exploration and Exploitation in Uncertain Environments" (PRIN PNRR 2022 fund, ID P2022EXP2W, CUP D53D23016020001).

* Corresponding author.
E-mail addresses: rongweiandrea.wu@mail.polimi.it (A. Wu), andresfelipe.cordoba@polimi.it (A. Cordoba-Pacheco), senem.ozgen@polimi.it (S. Ozgen), fredy.ruiz@polimi.it (F. Ruiz).

https://doi.org/10.1016/j.jprocont.2026.103638
Received 30 July 2025; Received in revised form 19 December 2025; Accepted 19 January 2026
Available online 27 January 2026

inputs and outputs, making them adaptable to different plant configurations, such as variations in reagents, injection techniques, or the number of abatement stages [14,15]. This modeling strategy is particularly effective for capturing the behavior of highly nonlinear and complex systems like acid gas abatement in WtE plants.

Alongside improvements in process modeling, there has been an increasing focus on the control and optimization of WtE operations to ensure compliance with strict emission regulations and minimize reagent consumption [16]. Among the advanced control strategies explored, Model Predictive Control (MPC) has emerged as a promising solution [17]. However, given the variable and uncertain dynamics of WtE systems, it is necessary to explore alternative modeling approaches that enhance MPC's robustness and adaptability.

Recent studies have explored the integration of data-driven modeling with MPC to enhance control performance. For example, [18] developed a dual long short-term memory (DLSTM)-based MPC to improve combustion efficiency and reduce nitrogen oxides (NOx) emissions. Similarly, [19] applied an MPC strategy using a backpropagation neural network (BPNN) to regulate furnace temperature in municipal waste incineration. In the context of acid gas abatement, [20] evaluated four MPC schemes for a two-stage system, showing that sorbent usage could be reduced by up to 60% compared to baseline controllers, under simulation conditions with linear models. To further manage uncertainty and process variability, [21] introduced a multi-model predictive control (MMPC) framework that employs a switching mechanism to adapt to changing operational conditions.

Given the challenges in identifying accurate dynamic models for WtE systems, the Set-Membership (SM) data-driven approach offers a robust alternative, especially when working with data from closed-loop systems. Unlike traditional statistical methods, it does not require independence between noise and input signals, a common assumption that is often violated in feedback controlled processes. Instead, it assumes unknown but bounded noise, which allows for the construction of a set of models consistent with observed data, providing a more reliable representation under uncertainty.

Building on this, the present work proposes a learning-based MPC strategy to regulate HCl concentration in the flue gas of a WtE plant by manipulating the reactant feed rate. A SM identification technique is integrated into the controller to enable online model adaptation, addressing the limitations of time-invariant models that may fail to capture dynamic changes caused by plant aging or operational modifications. Importantly, the proposed control framework also reflects realistic environmental regulation practices by enforcing average-based emission constraints over a defined time window, rather than imposing instantaneous limits at every control step, as commonly seen in the literature. This better aligns the control strategy with regulatory norms and allows more practical and flexible operation [22]. The approach is validated using experimental data from a real WtE facility in Italy, with the goal of ensuring emission compliance while minimizing reagent usage.

2. System and process description

This section provides an overview of the acid gas abatement process in the WtE plant. It describes the configuration and operational procedures of the plant to offer a clear understanding of how the system is structured and how acid gas treatment is integrated into the overall process.

The flue gas treatment system in the Waste-to-Energy (WtE) plant is shown in Fig. 1. It is designed to clean the flue gas generated during waste incineration before it is released into the atmosphere.

The process begins with the waste incineration unit, where solid waste is combusted to produce energy. The resulting flue gas, containing a mixture of pollutants, flows into a quencher to reduce its temperature. This cooling step also serves as the point where chemical reactants, such as bicarbonate and activated carbon, are injected into the gas stream.

As the flue gas progresses through the system, the acidic compounds, micro-pollutants, and heavy metals are neutralized through dry chemical reactions with the injected reagents. The gas then passes through a baghouse filter, which captures solid particulate matter. Further downstream, a Selective Catalytic Reduction (SCR) system removes NOx, ensuring the fulfillment of the environmental emission standards.

Finally, the cleaned flue gas is released into the atmosphere through the stack. To monitor the effectiveness of the acid gas abatement process, continuous HCl concentration sensors are installed both upstream and downstream of the treatment line, as shown in Fig. 1.

The acid gas abatement process is characterized by three key measured variables:

- The input acid concentration, denoted as HCl_{in}, is measured in the flue gas exiting the combustion chamber, and it represents a measured disturbance input to the control system d, as it directly influences the neutralization demand. This variable exhibits substantial variability due to the heterogeneity of the combusted waste material, as also documented in the literature [23,24].
- The output acid concentration, HCl_{out}, is measured at the stack and serves as the controlled variable y. It reflects the effectiveness of the abatement process and must remain within regulatory limits.
- The bicarbonate feed rate, $NaHCO_3$, is injected at the quencher stage and acts as the manipulated variable u. This is the main control input used to reduce the acid concentration in the flue gas.

Table 1
Main process variables for acid abatement during regular operation.

	Max	Min	Mean	Median	Std
HCl_{out} (mg/m^3)	46.0	0.004	4.7	4.5	2.0
HCl_{in} (mg/m^3)	3150	0.3	1211	1137	471
$NaHCO_3$ (kg/h)	2388	100	273	236	159
$Flowrate$ (m^3/h)	110 628	44 345	90 811	92 390	11 457

The dataset used in this work was collected from a full-scale WtE plant located in Italy, where the system operates under a traditional control strategy based on a combined feedback and feedforward configuration. The process variables were extracted from the Decentralized Control System (DCS) with a 1-minute sampling time, which is enough to regulate the output acid concentration, assess the abatement performance, and verify compliance with the regulatory emission limits. The data acquisition covered 52 days of regular operations, resulting in 74,880 samples gathered in a closed-loop configuration.

To ensure that the data accurately reflects the system's operational behavior, a pre-processing step was applied to inspect the dataset and remove invalid intervals, such as those corresponding to sensor calibration or Other Than Normal Operating Conditions (OTNOC). Table 1 summarizes the main characteristics of the filtered dataset. After preprocessing, the new dataset D contains 72,245 valid samples remaining available for analysis.

2.1. Abatement process model and control

To effectively design and implement control strategies for acid gas treatment, it is necessary to understand the chemical reactions and the role of the process variables in the neutralization dynamics. This study concentrates on HCl rather than other acid species, including SO_2 and HF, which also contribute to the emissions from waste combustion. Based on the dataset under consideration, the other two acid species occur less frequently at elevated concentrations and therefore do not pose significant challenges for their removal. Moreover, their contribution in terms of molar concentration is comparatively limited and

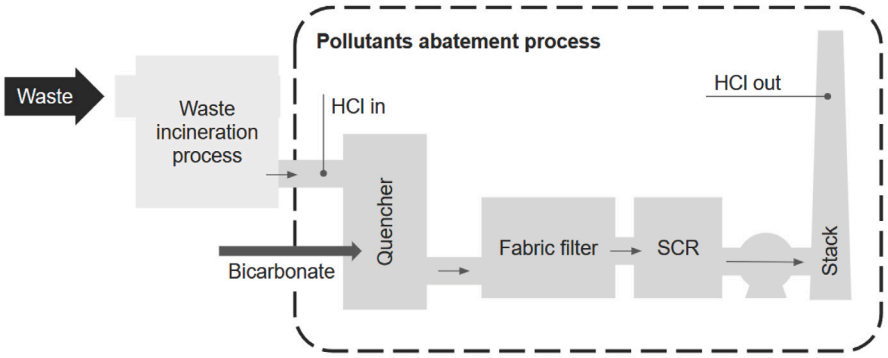

Fig. 1. WtE plant scheme, with bicarbonate-based acid abatement system.

sometimes negligible. On average, they form less than 3% of the total acid species present in the flue gas. Accordingly, emphasis is placed on HCl, as the principal acid species, given that its continuous presence and dominant molar contribution make it the most consequential target for investigation and optimization of its abatement strategies.

The abatement process consists of a chemical neutralization reaction between the acid gas and a base reagent, which can be generically described as

$$HCl + NaHCO_3 \Rightarrow NaCl + H_2O + CO_2 \tag{1}$$

where HCl is the acid and $NaHCO_3$ is the base reagent that react to produce a neutral compound in the form of sodium chloride (NaCl), water (H_2O), and carbon dioxide (CO_2) as byproducts. Based on stoichiometry considerations, 1 mole of $NaHCO_3$, is required to neutralize 1 mole of HCl. When expressed in mass terms, this corresponds to 2.3 kg of $NaHCO_3$ for 1 kg of HCl. This ratio serves as a baseline reference for neutralization in standard control strategies, with an additional gain factor typically applied to account for variations in reagent efficiency and specific plant configurations to ensure adequate acid removal.

In standard automation systems, the output concentration of HCl is regulated using a combined feedforward and feedback control strategy described as

$$u(t) = K_{FF}d(t) + R_{PID}(z)(y_{\text{ref}} - y(t)) \tag{2}$$

where $u(t)$ is the manipulated variable ($NaHCO_3$), K_{FF} represents the stoichiometric ratio which is scaled by the disturbance input $d(t)(HCl_{in})$, $R_{PID}(z)$ is the feedback controller, typically a PI or PID regulator, and y_{ref} is the set point for the desired output acid gas concentration. Additional control features such as actuator saturation and an anti-windup mechanism are implemented in practice but omitted from Eq. (2) for clarity.

3. Nominal MPC

This section presents the structure of the nominal MPC strategy used as the basis for the control framework developed in this work. The goal is to clarify how the optimization problem is structured and how system constraints are incorporated, specifically for the WtE plant described in Section 2.

The control strategy is formulated as a finite-horizon optimization problem subject to dynamic and operational constraints. Particular attention is paid to enforcing realistic environmental constraints rather than applying strict emission limits at each time step. The controller considers average-based constraints over a time window defined to reflect the averaging periods mandated by environmental regulations for emission limits. This formulation allows a practical and flexible implementation that reflects how emission limits are regulated in actual WtE plant operations.

The Integrated Environmental Authorization (IEA) establishes emission limit values based on environmental regulations specific to WtE plants. In particular, the acid gas abatement process must comply with strict emission limits, such as half-hourly average concentration limits for many pollutants present in the flue gas, which also include the HCl concentration, and these values are aligned with national environmental regulations [22].

In order to reflect these regulatory requirements, the proposed MPC formulation incorporates two types of constraints: hard emission limits, which must never be violated, and soft emission limits, which allow occasional exceedances under specific operational conditions. These constraints are formulated over the prediction horizon using average-based expressions, allowing the controller to respect both hard and soft emission limits as defined by regulatory standards.

To enforce the hard constraint, a cumulative limit is applied over the prediction horizon. This ensures that the average HCl concentration remains below the maximum allowed threshold as

$$\frac{1}{N}\sum_{i=0}^{N-1} y(i) \le \bar{y}_{\max} \qquad i \in [0, N]_{\mathbb{Z}} \tag{3}$$

where $y(i)$ is the predicted HCl concentration at the corresponding time step, N is the prediction horizon length, and $\bar{y}_{\max}$ represents the regulatory hard limit for the average HCl emission over the horizon.

In addition to the hard limit, a soft emission constraint is introduced to guide the system toward more conservative operation. This constraint is based on a lower threshold $\bar{y}_{\text{soft}}$, which provides a more restrictive target for average emissions while still allowing limited and controlled flexibility through a slack variable ζ_2 as,

$$\frac{1}{N}\sum_{i=0}^{N-1} y(i) \le \bar{y}_{\text{soft}} + \zeta_2 \qquad i \in [0, N]_{\mathbb{Z}} \tag{4}$$

here, ζ_2 is a slack variable that allows occasional violations of the soft limit when necessary to maintain feasibility and performance. This approach allows the controller to explore a broader solution space, especially under challenging process conditions, while still ensuring that emissions remain bounded by the hard legal limit defined in Eq. (3).

To support asymptotic convergence to the desired operating point, a terminal constraint is imposed on the output at the final step of the prediction horizon,

$$y_{\text{ref}} - \zeta_1 \le y(N) \le y_{\text{ref}} + \zeta_1 \tag{5}$$

here, y_{ref} is the design parameter representing the desired reference concentration at steady state, and ζ_1 is the slack variable defining a tolerance band around the target value. This ensures that the optimization remains feasible, especially under uncertain or variable conditions. To ensure valid solutions, the introduced slack variables are constrained to be non-negative,

$$\zeta_k \geq 0, \quad k \in \{1, 2\} \tag{6}$$

In addition, control signal constraints are enforced through standard actuator saturation limits,

$$u_{\min} \leq u(i) \leq u_{\max}, \quad \forall i \in [0, N]_{\mathbb{Z}} \tag{7}$$

where $u_{\min}$ and $u_{\max}$ represent the lower and upper bounds of the reactant feed rate.

Linear models have been widely used in industrial applications, as demonstrated in the literature [3,20]. The prediction model is chosen to follow an autoregressive model with exogenous inputs (ARX) structure, identified using historical data from a real Waste-to-Energy (WtE) plant located in Italy. This structure allows future output values to be related to past outputs, control actions, and measured disturbances, with an additive noise term,

$$\hat{y}(i) = \theta(i)'\varphi(i) + \varepsilon(i), \quad i = 1, \dots, N \tag{8}$$

where, $\theta \in \mathbb{R}^n$ is the model parameter vector and φ is the regressor vector defined as,

$$\varphi(i) = [\varphi^y(i)' \ \varphi^u(i)' \ \varphi^d(i)']'$$

where

$$\varphi^y(i) = [y(i-1) \dots y(i-na)]'$$
$$\varphi^u(i) = [u(i-1) \dots u(i-nb_1)]'$$
$$\varphi^d(i) = [d(i-1) \dots d(i-nb_2)]'$$
$$i \in [0, N]_{\mathbb{Z}}$$

In this formulation, the initial conditions for φ^y, φ^u, φ^d are given by,

$$\varphi^y(0) = [\text{HCl}_{out}(t-1) \dots \text{HCl}_{out}(t-na)]' \tag{9}$$
$$\varphi^u(0) = [\text{NaHCO}_3(t-1) \dots \text{NaHCO}_3(t-nb_1)]' \tag{10}$$
$$\varphi^d(0) = [\text{HCl}_{in}(t-1) \dots \text{HCl}_{in}(t-nb_2)]' \tag{11}$$

with na, nb_1, nb_2 representing the number of past output, control, and disturbance terms included in the regressor, respectively. A one-step delay is assumed between the output and both the control and disturbance inputs.

Finally, the disturbance input is assumed to remain constant over the prediction horizon as,

$$d(i) = \text{HCl}_{in}(t) \tag{12}$$
$$i \in [0, N]_{\mathbb{Z}}$$

where $\text{HCl}_{\text{in}}(t)$ represents the most recent measurement of the incoming acid concentration. This assumption simplifies the prediction model while still capturing the dominant effect of the disturbance on system behavior.

After describing the constraints of the nominal MPC, the proposed control strategy is formulated as a Quadratic Programming (QP) problem, where a quadratic cost function is minimized subject to linear dynamic and operational constraints over a specified prediction horizon N. The objective is to achieve accurate set-point tracking of the flue gas HCl concentration while ensuring regulatory compliance and minimizing reagent usage.

The first term in the cost function penalizes deviations of the predicted output $y(i)$ from the desired reference value y_{ref}, and is given by,

$$J_Q = \sum_{i=0}^{N} (y(i) - y_{\text{ref}})' Q_y (y(i) - y_{\text{ref}}) \tag{13}$$

Here, Q_y is a diagonal weighting matrix that allows tuning the controller's emphasis on output accuracy. This term ensures that the predicted HCl concentration remains close to the desired setpoint throughout the prediction horizon.

In contrast to standard MPC formulations that penalize only the magnitude of the control input, the proposed strategy incorporates process-specific knowledge by introducing a stoichiometric reference u_{stoich}. This reference represents the equilibrium feed rate required to neutralize the incoming acid load based on chemical stoichiometry, i.e., $u_{\text{stoich}} = K_{FF}\text{HCl}_{in}(t)$. The control input $u(i)$ is then penalized relative to this equilibrium point, rather than relative to zero, to explicitly discourage both over-dosage and under-dosage of the reagent:

$$J_R = \sum_{i=0}^{N-1} (u(i) - u_{\text{stoich}})' R (u(i) - u_{\text{stoich}}) \tag{14}$$

where R is a positive definite weighting matrix that regulates the cost associated with deviations from stoichiometric balance. This formulation reduces reagent waste and avoids unnecessary oscillations in the control action, which might arise from attempts to overcompensate for predicted disturbances in the feedforward path.

Finally, to ensure that the constraint violations remain limited and only occur when strictly necessary, the slack variables ζ_1 and ζ_2, introduced in the terminal and soft emission constraints, are penalized in the cost function. A linear penalty is applied to discourage the use of slack while preserving feasibility in scenarios where the constraints might otherwise be infeasible,

$$J_\zeta = \sum_{k=1}^{2} \rho \zeta_k \tag{15}$$

The penalty weight $\rho \in \mathbb{R}^+$ defines the cost of violating the corresponding constraint. This term ensures that the optimizer prioritizes constraint satisfaction but allows limited violations when necessary.

Moreover, based on the constraints and cost terms presented above, the nominal MPC optimization problem is formulated as

$$\begin{aligned} \underset{u(i),\zeta_k}{\text{minimize}} \quad & J_Q + J_R + J_\zeta \\ \text{subject to} \quad & (3), (4), (5), (6), (7), \\ & (8), (9), (10), (11), (12) \end{aligned} \tag{16}$$

The objective of the MPC is to repeatedly solve an optimization problem over a prediction horizon in order to compute the optimal bicarbonate feed rate. At each time step, only the first input of the computed control sequence is applied, and the optimization is solved again at the next step using updated process measurements.

It is important to note that solving the MPC problem in (16) requires an accurate prediction model. Since the true system dynamics are unknown and subject to variability, the prediction model is defined in the ARX form as given in (8). To ensure reliable prediction performance, a learning-based ARX approach is proposed to estimate and update the model parameters online using process data.

4. Learning-based MPC using set-membership approach

Based on the MPC formulation described in Section 3, the control objective remains to optimize the use of the reagent while maintaining the acid gas concentration close to its reference value and ensuring adherence to emission limits. However, to address dynamic variability caused by plant aging or changes in operating conditions, a SM estimation scheme is proposed, which recursively refines the model parameter set θ in the ARX structure using operational data collected during closed-loop execution. This learning-based strategy

enables the controller to adapt to evolving system dynamics in a data-driven approach.

4.1. Set-membership model adaptation

Considering that the prediction model used in the MPC formulation is based on an ARX structure, as described in (8), its selection reflects a trade-off between model accuracy and computational complexity. The model must be able to reliably forecast the system's short-term behavior, particularly the acid gas concentration within the prediction horizon, while also remaining simple enough to allow real-time optimization. This balance is crucial in WtE plants, where fast-changing dynamics and tight environmental constraints require both responsiveness and robustness in control [4,7,11,12].

Since the model is identified from a real industrial WtE plant, data collection must occur under closed-loop operation due to the safety-critical nature of the process and strict emission regulations. Performing open-loop experiments is impractical and potentially dangerous, as it may lead to constraint violations and operational inefficiencies. As a result, the collected data typically does not satisfy the statistical assumptions required by classical system identification techniques. To address these limitations, the SM framework is adopted, offering an alternative that does not rely on these assumptions.

In the SM framework, the model uncertainty is described using an Unknown But Bounded (UBB) noise signal ε, which satisfies $\|\varepsilon(t)\| \leq \epsilon$, where ϵ is a known upper bound on the noise. Let $\tilde{y}(t)$ and $\varphi(t|t-1)$ denote samples of output and regressor vectors from the dataset D, for times $t = 0$ to $t = M$. Based on the ARX model structure and the noise assumption, the Feasible Parameter Set (FPS) is the set that includes all parameter vectors that are consistent with data and the noise bound, given by

$$FPS = \left\{\theta \in \Theta : \left\|\tilde{y}(t) - \theta'\varphi(t|t-1)\right\| \leq \epsilon\right\} \quad \forall t \in [0, M]_{\mathbb{Z}} \tag{17}$$

To ensure that the FPS is non-empty, the smallest admissible noise bound ϵ is determined such that $FPS \neq \emptyset$, that is, there exist some values of θ that are consistent with the available information.

Once ϵ has been identified, the bounds of the parameter set are computed by solving two optimization problems for each parameter component θ_j, using a tolerance factor α, commonly set to 10% as suggested in [25].

$$\overline{\theta_j} = \arg\max_{\theta \in FPS} \quad \theta_j \quad \text{subject to} \quad \left\|\tilde{y} - \theta'\varphi\right\|_p \leq \epsilon\alpha, \tag{18}$$

$$\underline{\theta_j} = \arg\min_{\theta \in FPS} \quad \theta_j \quad \text{subject to} \quad \left\|\tilde{y} - \theta'\varphi\right\|_p \leq \epsilon\alpha, \tag{19}$$

The nominal model parameters $\hat{\theta}$ used in the MPC prediction are computed as the Chebyshev center of the resulting interval, $\hat{\theta}_j = \frac{\overline{\theta}_j + \underline{\theta}_j}{2}$.

The estimated parameter vector $\hat{\theta}$ is used to update the prediction model within the MPC formulation described in Section 3. However, the model is not updated at every control step; instead, it is periodically refined using a batch of W new samples collected during closed-loop operation. This learning-based update enables the controller to adapt to evolving system dynamics while preserving feasibility and optimizing control performance.

By leveraging the simplicity of the ARX structure and the convexity of the feasible parameter set, the SM estimation scheme remains computationally efficient and practical for deployment in industrial WtE settings. This adaptive control strategy enhances robustness against model mismatch and supports long-term operation under varying conditions.

5. Simulation environment and experimental setup

This section outlines the simulation environment and testing conditions used to evaluate the performance of the proposed control strategy. To this end, the dataset D is subdivided into two parts: a training set, consisting of 15 days of operational data (approximately 22,000 samples), and a validation set, comprising the remaining 50,245 samples, as graphically illustrated in Fig. 2. This partitioning ensures that model development and controller validation are performed on disjoint data, minimizing bias and improving the reliability of the evaluation.

Conducting real-time control experiments on WtE plants is often impractical due to safety considerations, strict regulatory constraints, and the risk of disrupting continuous operations. To address these limitations, a simulation model is employed to replicate the dynamic behavior of the plant and enable offline testing of the proposed control strategy.

A Hammerstein-Wiener (HW) model structure is adopted for this purpose, as it is well-suited to capture the nonlinear input–output relationships typical of WtE processes, as demonstrated in [26]. This model combines static nonlinear blocks with a linear dynamic core, offering the flexibility needed to represent complex process behavior while maintaining a tractable structure. Its nonlinear formulation successfully captures the long-term behavior of the process, providing strong performance with a limited number of parameters.

The HW model is based on an ARX structure, assuming an additive noise signal that affects only the output, without influencing the autoregressive component. In addition, static nonlinearities are applied to both the input and output signals of the process, expressed as,

$$\begin{aligned} w_m(t) &= l\left(u_m(t), \sigma\right); \quad m = 1, \ldots, M \\ x_m(t) &= \sum_{i=1}^{na_m} f_{im} x_m(t-i) + \sum_{m=1}^{M}\sum_{j=0}^{nb_m} b_{mj} w_m(t-j) \\ y(t) &= h\left(\sum_{m=1}^{M} x_m(t), \sigma\right) + e(t) \end{aligned} \tag{20}$$

In this formulation, $l(\cdot, \sigma)$ and $h(\cdot, \sigma)$ represent the static nonlinear input and output functions, respectively, both parameterized by σ. The term $w_m(t)$ denotes the transformed input signals after passing through the input nonlinearity block. These inputs are then processed by a linear dynamic component, which governs the system's internal evolution before the output nonlinearity is applied. The hyperparameters of the model include the regressor lengths na_m, nb_m, and the function families used to represent the nonlinearities $l(\cdot, \sigma)$ and $h(\cdot, \sigma)$.

The hyperparameters of the ARX model, which also define the linear dynamic component of the HW structure, are selected as $na = [3, 3]$, $nb = [3, 3]$. This configuration ensures a sufficient dynamic order to capture the system behavior while maintaining model simplicity. In the configuration adopted for the HW configuration, the input nonlinearity is defined as an identity function $l(u) = u$, reflecting the approximately linear behavior of the actuator. For the output nonlinearity, a second-order polynomial is used to capture mild nonlinearities in the process output [26]. The performance of the identified models is evaluated using standard key performance indicators (KPIs) such as Mean Squared Error (MSE), Root Mean Squared Error (RMSE), Mean Absolute Error (MAE), and maximum absolute error ($E_{\max}$). The ARX model is evaluated both in k-step ahead prediction and in simulation, while the HW model is evaluated only in simulation. The obtained results are summarized in Table 2 and visually illustrated in Fig. 3.

After identifying and validating the nominal ARX model through the Set-Membership method of Section 4.1 and the nominal HW model through the prediction error method, the next step is to define the closed-loop simulation setup used to evaluate the control strategy. This setup is illustrated in Fig. 4. In this framework, the HW simulation model represents the process dynamics by taking as inputs the acid concentration in the flue gases from the incinerator phase, see Fig. 1, and the bicarbonate feed rate generated by the MPC strategy. This

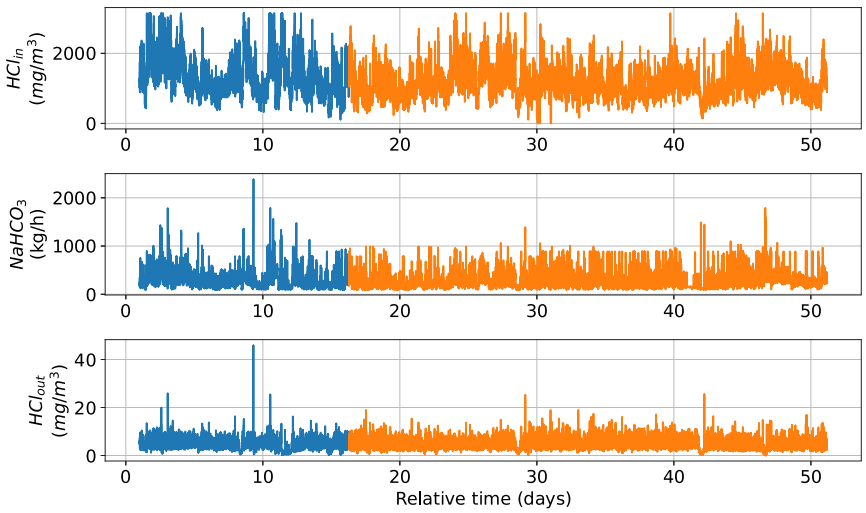

Fig. 2. Training (blue) and validation (orange) periods of the collected dataset.

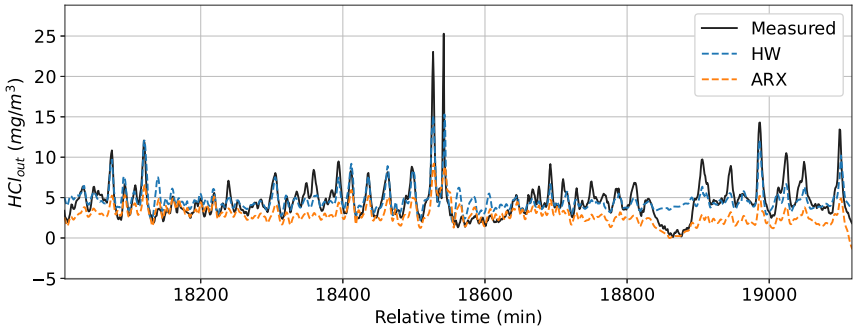

Fig. 3. Comparison of measured output (black) and concentrations evaluated in simulation for ARX (orange) and HW (blue) models.

Table 2
ARX and HW models performance.

	MSE	RMSE (mg/m^3)	MAE (mg/m^3)	E_{max} (mg/m^3)
ARX 1-step prediction	0.12	0.34	0.24	16.9
ARX 5-step prediction	1.83	1.35	0.98	18.0
ARX 15-step prediction	3.41	1.87	1.41	16.3
ARX simulation	6.65	2.58	2.06	17.7
HW simulation	1.98	1.41	1.07	18.3

model is kept constant throughout the entire simulation campaign. The model outputs the resulting acid gas concentration, which, along with other process variables, is fed back into the adaptive MPC scheme.

The controller solves a Finite Horizon Control Optimization Problem (FHCOP) using the identified ARX system as prediction model, which is periodically updated with new measurements. The effectiveness of the control strategy depends not only on external design choices but also on how frequently new data are accumulated and used to refine the prediction model. The prediction model is initialized using a batch of data collected during a time window equal to the adaptation period, which defines how often the model is retrained during closed-loop operation.

The entire control framework was implemented in Python using the `cvxpy` library [27] for formulating the optimization problem, and the `OSQP` solver [28] for efficiently solving the resulting quadratic programming problem. The development of the HW simulation model structure was built using `NumPy` for numerical operations and matrix handling [29].

6. Results

This section presents the evaluation of the proposed adaptive MPC strategy, based on the system models developed in the previous sections. A comparative analysis is conducted between three configurations: (i) the existing closed-loop PID operational data from the physical WtE plant, (ii) simulation results using a baseline controller applied to the HW model, and (iii) simulation results using the proposed Adaptive MPC strategy. The evaluation covers a two-week period of continuous operation, with system data sampled at one-minute intervals to enable high-resolution performance assessment.

To assess the effectiveness of the adaptive modeling approach, Fig. 5 compares the evolution of the average interval of the FPS (FPI) under different model update frequencies. The update batches contain W samples (180, 360, 720 and 1440 1-minute measurements) collected respectively in the last 3, 6, 12 and 24 h, depending on how frequently the model is updated using the newly acquired data. Short update periods, such as 3 h, lead to fast convergence of the parameter bounds due to the use of smaller data windows. While this can accelerate adaptation, it also increases the risk of overfitting and reduces generalization capability. In contrast, longer update intervals (e.g., 6 or 12 h) allow the model to incorporate more data before each update, resulting in more stable parameter estimates and improved predictive performance. However, long adaptation windows, such as 24 h, can degrade accuracy during the early stages of adaptation. This is reflected in higher RMSE values, highlighting the trade-off between fast responsiveness and model estimation accuracy.

Based on the previous analysis, Fig. 6 compares the adaptive modeling approach against the non-adaptive one. Both models are initialized with the same parameter values obtained from the initial batch of

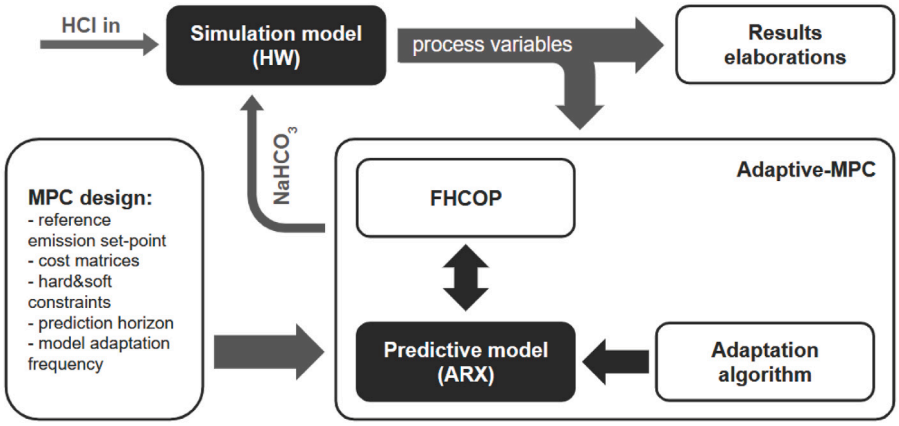

Fig. 4. MPC simulation scheme.

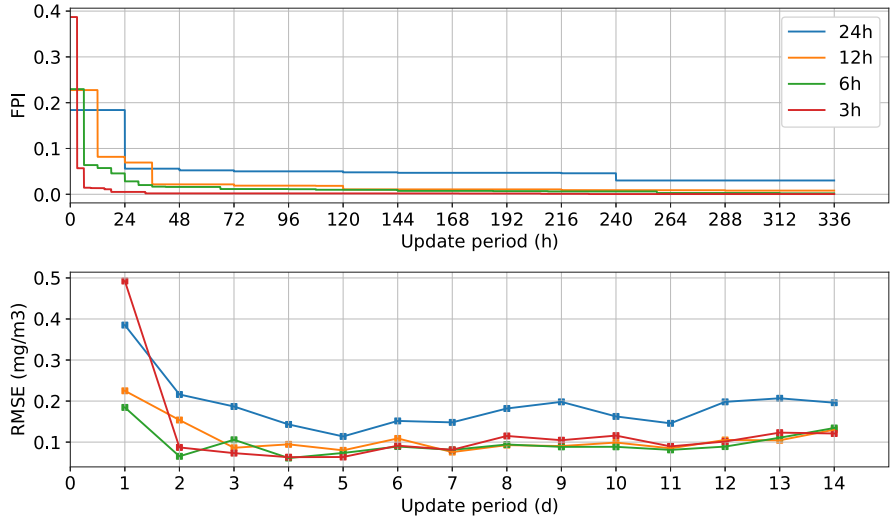

Fig. 5. ARX model adaptation: average interval of the feasible parameter set (top) and 1-step prediction RMSE over each adaptation period (bottom)

training data. However, the adaptive ARX model updates its parameters every 6 h using new measurements, while the non-adaptive model continues with its initial parameters throughout the simulation. The figure describes how the adaptive model progressively refines its predictions by reducing the width of the FPI and improving its 1-step prediction accuracy, as indicated by the decreasing RMSE.

With the adaptive model structure and update mechanism established, the next step is to define the MPC controller settings used in the simulation. Table 3 summarizes the main parameters employed in the control problem formulation, including the reference value, cost weighting factors, and constraint thresholds.

In accordance with regulatory requirements [22], the daily average concentration limit is assigned to the y_{ref} parameter, representing the long-term target concentration level at which the plant is expected to operate. The half-hourly concentration thresholds stipulated by the regulation are assigned to the parameters $\bar{y}_{\text{soft}}$ and $\bar{y}_{\text{max}}$. The value $\bar{y}_{\text{soft}}$ denotes an intermediate attention threshold that permits a limited number of exceedances throughout the plant's annual operation, while $\bar{y}_{\text{max}}$ corresponds to a critical upper limit. Surpassing this limit indicates a serious regulatory violation and may trigger emergency shutdown procedures. The physical limitations of the reagent feeder are considered through the saturation values u_{min} and u_{max} that indicate the real operating range, based on the minimum and maximum dosage, for the reagent feeder tasked with injecting the reagent in the quencher. These parameters are kept constant across all scenarios to ensure a fair and consistent comparison.

Table 3
MPC configuration parameters.

Parameter	Value	Unit
y_{ref}	5	mg/Nm^3
N	30	–
Q_y	4	–
R	0.01	–
ρ	0.1	–
$\bar{y}_{\text{soft}}$	10	mg/Nm^3
$\bar{y}_{\text{max}}$	30	mg/Nm^3
u_{min}	100	kg/h
u_{max}	1000	kg/h

In addition to the real plant data, a baseline control strategy is introduced as a simulation-based reference for assessing the performance improvements achieved by the proposed adaptive MPC approach. The baseline scheme consists of a FeedForward and FeedBack (FF+FB) configuration, a structure commonly employed in acid gas abatement systems.

Given the absence of detailed process models required for advanced tuning methods, the feedback controller is tuned using the Ziegler–Nichols method, a widely adopted approach in industrial settings. This method offers practical performance across many processes and determines PID gains empirically by pushing the closed-loop system to the stability limit to estimate the ultimate gain and oscillation period.

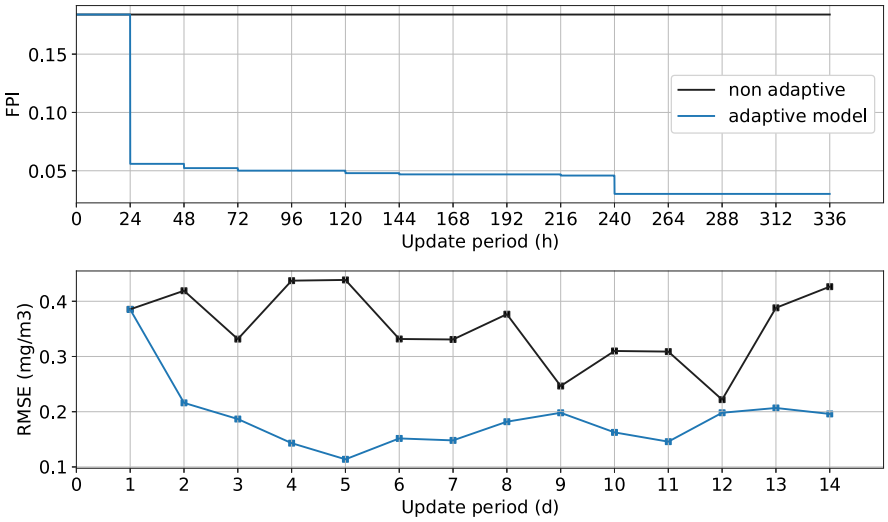

Fig. 6. Closed-loop performance comparison of MPC strategies using adaptive (blue) and static (black) ARX models.

Table 4
Control results, 2 weeks of simulation data.

	MIAE (mg/m^3)	MISE $(mg/m^3)^2$	Mean HCl_{out} (mg/m^3)	Mean $NaHCO_3$ (kg/h)
Plant data	1.4	3.4	4.5	250.3
$FF+FB$	0.9	1.7	4.6	253.1
MPC	0.6	0.7	4.5	242.6

Specifically, the ARX-based model is used to estimate the process time constant T and delay τ from the step response, which are then used to determine the controller gains.

To evaluate the performance of control systems, two standard tracking metrics are considered, the Mean Integral Absolute Error (MIAE) and the Mean Integral Squared Error (MISE), defined in (21) and (22), respectively

$$MIAE = \sum_{i=1}^{N} \frac{1}{N} |y_{ref}(i) - y(i)| \tag{21}$$

$$MISE = \sum_{i=1}^{N} \frac{1}{N} (y_{ref}(i) - y(i))^2 \tag{22}$$

Table 4 presents the tracking performance of the reference value across all control schemes, along with the mean emissions and average bicarbonate consumption. It is evident that the MPC significantly improves performance compared to both the real system and the FF+FB control, reducing the MIAE by 57.1% and 33.3%, and the MISE by 79.4% and 58.8%, relative to plant data and FF+FB controller results, respectively. Although the HCl_{out} values remain very similar across controllers, the MPC achieves a 3% reduction in $NaHCO_3$ consumption.

Although the mean value of $NaHCO_3$ consumption is not substantially reduced, the MPC demonstrates high performance in tracking the stoichiometric ratio, as shown in Fig. 7. The MPC closely follows the optimal feed rate, effectively minimizing both over-dosage and under-dosage of the reagent.

To further analyze system behavior under varying operating conditions, particularly considering the high variability of the disturbance input, Fig. 8 illustrates the trajectories of HCl_{in}, $NaHCO_3$, and HCl_{out} over a selected time window. It is observed that both the real plant and the baseline control scheme tend to induce under- or over-dosage conditions. These imbalances lead to emission peaks followed by aggressive corrective responses, ultimately resulting in unnecessary reagent consumption and inefficient operation, whereas the proposed control strategy reacts more effectively to such changes.

Some limitations of the simulation model become evident in scenarios with low HCl_{in} concentrations, as illustrated in Fig. 9. During the simulation period, there are short intervals in the dataset where the acid concentration in the flue gases is unusually low. In these cases, all the control actions tend to reach the lower saturation limit, potentially leading to overdosage situations. This effect is noticeable in the real dataset, where lower emission concentrations are achieved, while the simulation models tend to overpredict HCl_{out}. These discrepancies are observed during rare events with a duration of 1–2 h, which represent approximately 1200 min over the two-week evaluation period.

The reduced simulation accuracy in these segments may be attributed to the limited number of low-acid data points available during HW model training. Additionally, the semi-batch nature of the solid reactant is an important factor, since unreacted material may accumulate on the filter-bag surfaces between jet-pulse cleaning cycles. The supplementary reactivity provided by the deposited bicarbonate becomes relevant as the feed rate of new reactant diminishes and reaches the operational minimum. This phenomenon has been discussed in the literature, where very low feed rates in bicarbonate acid gas removal systems might exhibit an apparent high efficiency [30].

In addition to improving tracking performance and minimizing extreme control actions, the MPC strategy contributes to smoother actuator behavior. As shown in the boxplot Fig. 10, the MPC reduces both the peaks and variability of the bicarbonate feed rate compared to the other controllers. This helps to preserve actuator life and enhances overall system stability.

To reflect realistic environmental regulations, which enforce average-based emission limits over defined time windows using half-hourly averages as outlined in the Directive 2010/75/EU of the European Parliament and of the Council of 24 November 2010 on industrial and livestock rearing emissions [31], Fig. 11 presents a boxplot illustrating the distribution of performance measures. The variability in the real system's emissions ranges from 2 mg/m^3 to 7 mg/m^3, with a mean value of 4.8 mg/m^3, emissions with the FF+FB controller have a range between 3.5 mg/m^3 and 5.7 mg/m^3 with mean at 4.6 mg/m^3, while the proposed Adaptive MPC reduces the emissions variability to between 3.6 mg/m^3 and 5.4 mg/m^3, achieving the lowest mean value of 4.5 mg/m^3. The violations of the imposed soft limit to maintain the HCl_{out} below 10 mg/m^3 have been respected by both the control methods. However, the overruns above the imposed reference of 5 mg/m^3, evaluated on half-hourly averages, have been reduced by 25% with respect to the FF+FB strategy (108 instances, with max of 7.6 mg/m^3) by the MPC approach (81 instances, with max of 6.9 mg/m^3). This demonstrates the Adaptive MPC's superior ability to

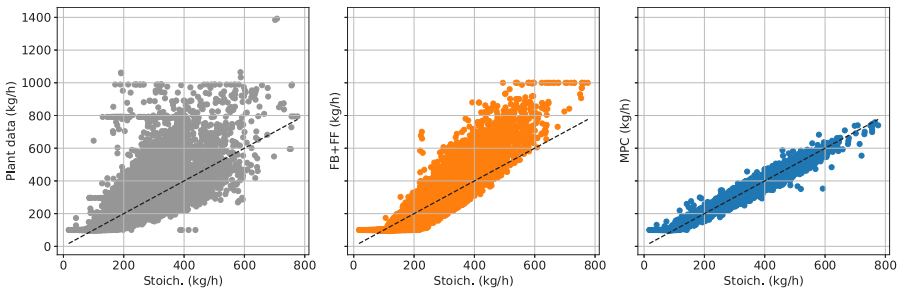

Fig. 7. Scatter plot comparisons of bicarbonate consumption with the ideal feed rates based on stoichiometry for experimental data (left), FF+FB controller (center), and MPC (right).

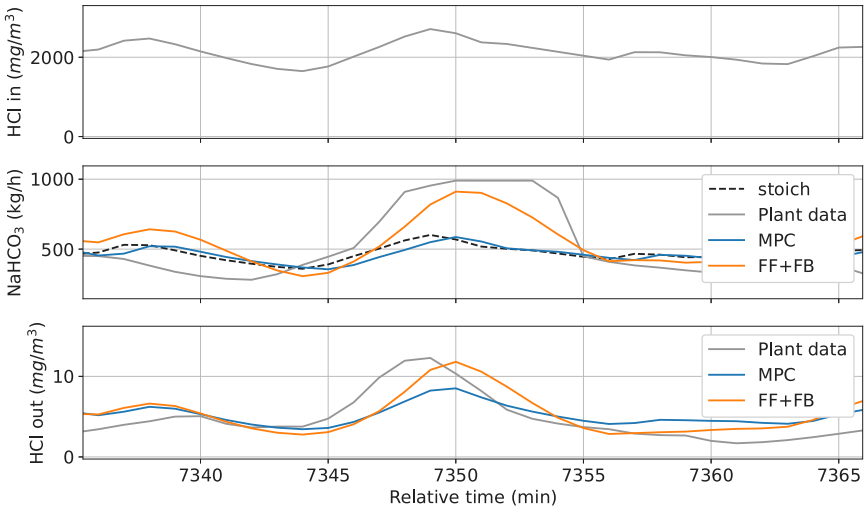

Fig. 8. Critical bicarbonate under- or over-dosage situation.

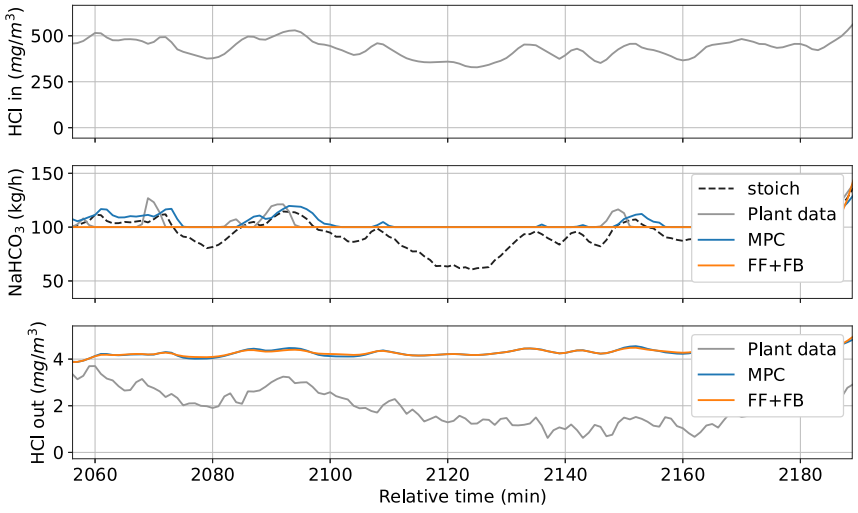

Fig. 9. Emission behavior during outlier low-acid concentration scenarios.

maintain emissions within stricter bounds consistent with regulatory requirements.

Finally, regarding computational time, the quadratic programming problem with linear constraints is solved efficiently, with each optimization step taking significantly less than one minute. In simulations, around 3680 optimization steps were completed within one minute. This provides a substantial margin for real-time implementation, as the MPC control action can be updated every minute, consistent with the simulation data frequency, without delays caused by solving the optimization problem. Therefore, the algorithm is well-suited for online regulation of systems with sampling periods on the order of minutes.

7. Conclusion

This paper presents a learning-based MPC strategy for regulating HCl emissions in Waste to Energy plants, employing real plant data. The limitations of time-invariant models are addressed through online model adaptation using Set-Membership identification, combined with

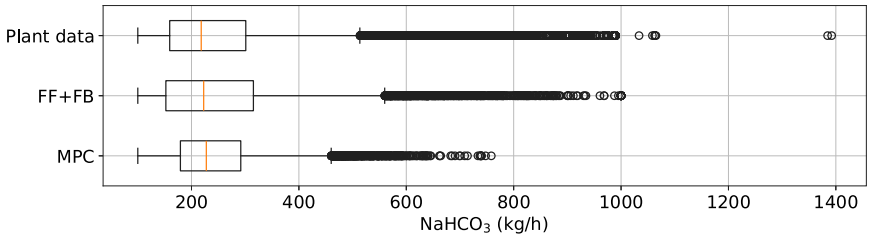

Fig. 10. Box plots comparison bicarbonate feed rates, process data and simulation results for MPC and conventional control structure (FF+FB)

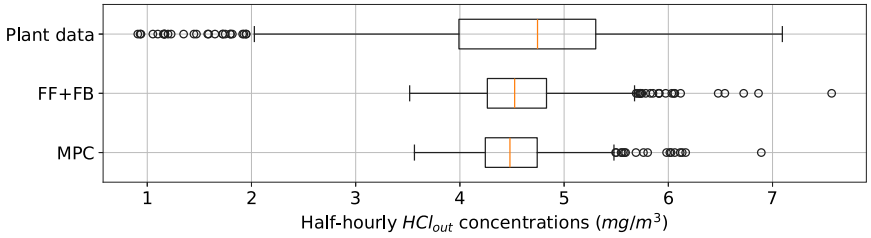

Fig. 11. Box plots comparison acid emissions, process data and simulation results for MPC and conventional control structure (FF+FB)

an MPC strategy, including time-windowed average constraints aligned with real-world environmental regulations.

The process demonstrates that adaptive models can significantly shorten the modeling phase for MPC implementation once a suitable model class is identified offline. This implies an improved controller performance, reducing the MIAE by up to 57.1% and the MISE by up to 33.3%, while also achieving a 3% reduction in average bicarbonate consumption. Nevertheless, some limitations in the available data may lead to suboptimal behavior at low concentration levels. Finally, the emission constraints incorporated in the optimization problem ensure better compliance with regulatory limits that cannot be directly enforced using conventional control schemes.

Future work will focus on enriching the dataset with operations at lower concentrations, possibly performing specific experiments to further leverage the adaptation technique. Furthermore, the approach could be extended to other acid species by developing simulation models for SO_2 and HF, using datasets that include events with higher concentrations of these pollutants in the flue gas. These extensions would provide tools to test and validate the proposed control framework under conditions where the assumption of HCl being the dominant acid species in the flue gas becomes less reliable.

CRediT authorship contribution statement

Andrea Wu: Writing – original draft, Visualization, Validation, Software, Investigation. **Andres Cordoba-Pacheco:** Writing – original draft, Visualization, Validation, Software, Methodology, Investigation, Formal analysis, Conceptualization. **Senem Ozgen:** Writing – review & editing, Visualization, Supervision, Resources, Methodology, Investigation, Formal analysis, Conceptualization. **Fredy Ruiz:** Writing – review & editing, Supervision, Resources, Methodology, Investigation, Formal analysis, Conceptualization.

Declaration of competing interest

The authors declare that they have no known competing financial interests or personal relationships that could have appeared to influence the work reported in this paper.

Data availability

Data will be made available on request.

References

[1] A.H. Khan, E.A. López-Maldonado, S.S. Alam, N.A. Khan, J.R.L. López, P.F.M. Herrera, A. Abutaleb, S. Ahmed, L. Singh, Municipal solid waste generation and the current state of waste-to-energy potential: State of art review, Energy Convers. Manage. 267 (2022) 115905, http://dx.doi.org/10.1016/j.enconman.2022.115905.

[2] H. Ding, J. Qiao, W. Huang, T. Yu, Cooperative event-triggered fuzzy-neural multivariable control with multitask learning for municipal solid waste incineration process, IEEE Trans. Ind. Inform. 20 (2024) 765–774, http://dx.doi.org/10.1109/TII.2023.3264108.

[3] A. Yan, K. Hu, Data-driven multitarget online modeling of the municipal solid waste incineration process, IEEE Trans. Ind. Inform. 20 (2024) 14124–14133, http://dx.doi.org/10.1109/TII.2024.3441640.

[4] H. Duan, X. Meng, J. Tang, J. Qiao, Dynamic system modeling using a multi-source transfer learning-based modular neural network for industrial application, IEEE Trans. Ind. Inform. 20 (2024) 7173–7182, http://dx.doi.org/10.1109/TII.2023.3342896.

[5] G. Antonioni, F. Sarno, D. Guglielmi, P. Morra, V. Cozzani, Simulation of a two-stage dry process for the removal of acid gases in a mswi, Chem. Eng. Trans. 24 (2011) 1063–1068, http://dx.doi.org/10.3303/CET1124178.

[6] O. Levenspiel, Chemical Reaction Engineering, Wiley, 2015.

[7] F.G. Ortiz, P. Ollero, Modeling of the in-duct sorbent injection process for flue gas desulfurization, Sep. Purif. Technol. 62 (2008) 571–581, http://dx.doi.org/10.1016/j.seppur.2008.03.012.

[8] C.E. Weinell, P.I. Jensen, K. Dam-Johansen, H. Livbjerg, Hydrogen chloride reaction with lime and limestone: kinetics and sorption capacity, Ind. Eng. Chem. Res. 31 (1992) 164–171, http://dx.doi.org/10.1021/ie00001a023.

[9] A. Dal Pozzo, R. Moricone, G. Antonioni, A. Tugnoli, V. Cozzani, Hydrogen chloride removal from flue gas by low-temperature reaction with calcium hydroxide, Energy & Fuels 32 (2017) 747–756, http://dx.doi.org/10.1021/acs.energyfuels.7b03292.

[10] R.J. Giraud, P.H. Taylor, R.B. Diemer, C.-P.H. and, Design and qualification of a bench-scale model for municipal waste-to-energy combustion, J. Air Waste Manage. Assoc. 72 (2022) 849–875, http://dx.doi.org/10.1080/10962247.2022.2054879.

[11] B. Han, D. Kumar, Y. Pei, M. Norton, S.D. Adams, S.Y. Khoo, A.Z. Kouzani, Modelling of thermochemical processes of waste recycling: A review, J. Anal. Appl. Pyrolysis 182 (2024) 106687, http://dx.doi.org/10.1016/j.jaap.2024.106687.

[12] Y. Hou, Q. Wang, K. Zhou, L. Zhang, T. Tan, Integrated machine learning methods with oversampling technique for regional suitability prediction of waste-to-energy incineration projects, Waste Manage. 174 (2024) 251–262, http://dx.doi.org/10.1016/j.wasman.2023.12.006.

[13] L. Sabug, F. Ruiz, L. Fagiano, SMGO-Δ: Balancing caution and reward in global optimization with black-box constraints, Inform. Sci. 605 (2022) 15–42, http://dx.doi.org/10.1016/j.ins.2022.05.017.

[14] M. Ghasemi, M. Samadi, E. Soleimanian, K.-W. Chau, A comparative study of black-box and white-box data-driven methods to predict landfill leachate permeability, Environ. Monit. Assess. 195 (2023) 862, http://dx.doi.org/10.1007/s10661-023-11462-9.

[15] R. Bacci di Capaci, G. Pannocchia, A. Dal Pozzo, G. Antonioni, V. Cozzani, Data-driven models for advanced control of acid gas treatment in waste-to-energy plants, IFAC-PapersOnLine 55 (7) (2022) 869–874, http://dx.doi.org/10.1016/j.ifacol.2022.07.554.

[16] A. Dal Pozzo, G. Muratori, G. Antonioni, V. Cozzani, Economic and environmental benefits by improved process control strategies in hcl removal from waste-to-energy flue gas, Waste Manage. (2021) Pages 303–315, http://dx.doi.org/10.1016/j.wasman.2021.02.059.

[17] J. Tang, H. Tian, T. Wang, A review of model predictive control for the municipal solid waste incineration process, Sustainability 16 (2024) http://dx.doi.org/10.3390/su16177650.

[18] J. Sun, X. Meng, J. Qiao, Data-driven optimal control for municipal solid waste incineration process, IEEE Trans. Ind. Inform. 19 (12) (2023) 11444–11454, http://dx.doi.org/10.1109/TII.2023.3246467.

[19] B. Wang, J. Tang, H. Xia, H. Tian, T. Wang, Z. Wu, Furnace temperature control for mswi process based on neural network predictive controller, in: 2024 36th Chinese Control and Decision Conference, CCDC, 2024, pp. 1731–1736, http://dx.doi.org/10.1109/CCDC62350.2024.10587853.

[20] R. Bacci di Capaci, M. Vaccari, G. Pannocchia, Enhancing sustainability of acid gas treatment in a waste-to-energy plant via model predictive control, Clean. Prod. 410 (2023) http://dx.doi.org/10.1016/j.jclepro.2023.137222.

[21] M. Liu, X. Li, K. Wang, Z. Liu, G. Li, Multi-model predictive control of converter inlet temperature in the process of acid production with flue gas, Internat. J. Adapt. Control Signal Process. 38 (2024) 1725–1743, http://dx.doi.org/10.1002/acs.3774.

[22] D.Lgs. 152/06, Decreto legislativo 3 aprile 2006, testo unico ambientale, Gazz. Uff. N. 152, Parte IV (2006) https://www.gazzettaufficiale.it/dettaglio/codici/materiaAmbientale.

[23] W. Meynendonckx, M. Ishteva, M. Verbeke, N. Alderweireldt, J. De Greef, Impact of furnace and waste layer control on hcl and so2 in combustion gas from a grate-fired waste-to-energy boiler, Process. Saf. Environ. Prot. 193 (2025) 710–720, http://dx.doi.org/10.1016/j.psep.2024.11.051.

[24] A. Dal Pozzo, L. Lazazzara, G. Antonioni, V. Cozzani, Techno-economic performance of hcl and so2 removal in waste-to-energy plants by furnace direct sorbent injection, J. Hazard. Mater. 394 (2020) http://dx.doi.org/10.1016/j.jhazmat.2020.122518.

[25] M. Lauricella, L. Fagiano, Set membership identification of linear systems with guaranteed simulation accuracy, IEEE Trans. Autom. Control 65 (2020) 5189–5204, http://dx.doi.org/10.1109/TAC.2020.2970146.

[26] S. Ozgen, A. Wu, F. Ruiz, Modeling approaches for data-driven model predictive control of acid gases in waste-to-energy plants, Waste Manage. 204 (2025) 114902, http://dx.doi.org/10.1016/j.wasman.2025.114902.

[27] S. Diamond, S. Boyd, Cvxpy: A python-embedded modeling language for convex optimization, J. Mach. Learn. Res. 17 (2016) 1–5, http://jmlr.org/papers/v17/15-408.html.

[28] B. Stellato, G. Banjac, P. Goulart, A. Bemporad, S. Boyd, Osqp: An operator splitting solver for quadratic programs, in: 2018 UKACC 12th International Conference on Control, CONTROL, 2018, http://dx.doi.org/10.1109/CONTROL.2018.8516834, 339–339.

[29] C.R. Harris, K.J. Millman, S.J. van der Walt, R. Gommers, P. Virtanen, D. Cournapeau, E. Wieser, J. Taylor, S. Berg, N.J. Smith, R. Kern, M. Picus, S. Hoyer, M.H. van Kerkwijk, M. Brett, A. Haldane, J.F. del Río, M. Wiebe, P. Peterson, P. Gérard-Marchant, K. Sheppard, T. Reddy, W. Weckesser, H. Abbasi, C. Gohlke, T.E. Oliphant, Array programming with NumPy, 585, 2020, pp. 357–362, http://dx.doi.org/10.1038/s41586-020-2649-2,

[30] A. Dal Pozzo, M. Giannella, G. Antonioni, V. Cozzani, Optimization of the economic and environmental profile of hcl removal in a municipal solid waste incinerator through historical data analysis, Chem. Eng. Trans. 67 (2018) 463–468, http://dx.doi.org/10.3303/CET1867078.

[31] DIRECTIVE 2010/75/EU, Directive 2010/75/eu of the european parliament and of the council of 24 november 2010 on industrial and livestock rearing emissions (integrated pollution prevention and control) (recast), 2010, https://eur-lex.europa.eu/eli/dir/2010/75/2024-08-04.